ELSEVIER

Journal of Power Sources 61 (1996) 167–171

JOURNAL OF POWER SOURCES

Preparation and properties of small diameter tubular solid oxide fuel cells for rapid start-up

I.P. Kilbride

Centre for Inorganic Chemistry and Materials Science, Department of Chemistry, Keele University, Staffordshire ST5 5BG, UK

Abstract

The feasibility of producing solid oxide fuel cells (SOFCs) which could be rapidly heated to operating temperature was investigated. Small diameter (2.4 mm) 3 and 8 mol% yttria-stabilised zirconia (YSZ) tubes were used both as the electrolyte and the cell support tube. Cells were prepared by winding with pure silver, Ni80/Cr20 and Nimonic 90 wires over lanthanum–strontium–manganite (LSM) cathodes. Specific power outputs of up to 250 mA/cm^2 at 900 °C, 0.7 V were achieved in silver wound cells with 5 mm long cathodes. Longer cathodes produced progressively lower specific outputs. This was attributed to increasing cathode and winding resistance with length. The base metal windings achieved up to 80% of the performance of a similar length cell wound with pure silver wire. Silver wound cells were successfully cycled between 200 and 900 °C at an average 25 °C/min (peak 100 °C/min) over 50 cycles with no degradation due to the thermal cycling. Degradation in cells wound with base metals was attributable to the increase in contact resistance found between the cathode and the wire with time.

Keywords: Solid oxide fuel cell; Start-up properties

1. Introduction

Fuel cells are particularly attractive devices for energy production because they utilise a reversible chemical reaction directly, and as such, are not limited by the Carnot thermodynamic cycle. At their normal operating temperature, solid oxide fuel cells (SOFCs) are more efficient than a heat engine [1]. Thus they may be a suitable replacement for the internal combustion engine on efficiency alone. For an automotive application, efficiency is not the defining criterion. These tend to be cost, reliability, ease of manufacture, etc. SOFCs have not been investigated for use in automotive devices despite several inherent advantages. The high temperature (700 to 1000 °C) required to operate a SOFC allows, in principle, a wide variety of fuels to be utilised. The high grade waste heat and exhaust can be used to externally or preferably internally reform hydrocarbon fuels. However, conventional planar SOFC designs suffer from long start-up times because of the low thermal shock resistance of the SOFC materials. While this is not a disadvantage in a static power generation system, it seems unreasonable to run an automobile power source continuously.

The approach adopted in this study is to use traditional SOFC materials, yttria-stabilised zirconia as the electrolyte and the positive electrolyte negative (PEN) support, lanthanum–strontium–manganite (LSM) as the cathode and nickel–YSZ–cermet as the anode, but also to use smaller diameter tubes to achieve increased thermal shock resistance. Zirconia tubes of 3 mm outside diameter have been prepared successfully by extrusion which retain mechanical integrity after heating and cooling from 1000 °C in less than 1 min [2]. The use of small diameter tubes has other inherent advantages. Tubes resistant to thermal stresses can be manifolded external to the hot zone. This has the advantage that the fuel manifold can be made out of less exotic materials, such as polymers, and also removes the necessity for high temperature sealing. By using a metal wire wound over the cathode as a current collector (or interconnect), series or parallel electrical connections can also be made externally. Because the metal wire is supported by the YSZ tube, high temperature strength is irrelevant and metals such as silver, with its excellent electrical conductivity, can be used. It would be desirable, however, to replace silver with base metal superalloys. In this preliminary study, Nickel80/chrome20 (Ni/

PII S0378-7753(96)02362-2

Cr) and Nimonic 90 alloy wires are used as a model for more complex superalloys because of ease of availability.

2. Experimental

YSZ tubes of 2.4 mm outside diameter, 250 mm wall thickness were fabricated by extrusion (supplied by Sapco) from 3 and 8 mol% YSZ (Tosoh TZ3Y and TZ8Y).

An anode slip was prepared from 10.5 g NiO (Alfa Chemicals), 5 g YSZ (Unitec FYT11) calcined at 1500 °C and passed through a 108 mm sieve, 2.9 g 1,1,1-trichloroethane, 2.1 g methanol and 0.1 g glycerol trioleate milled for 3 h using zirconia media. 0.1 g polyvinyl butyral (Wacher BS18) was added 5 min before the end of milling. The slip was introduced immediately into the YSZ tubes using a syringe. The tubes were allowed to drain, leaving a thin coating of approximately 40 μm. The tubes were subsequently dried at 150 °C. The anode was fired at 1300 °C for 1 h.

The cathode electrochemical layer was applied using an LSM/ZrO_2 ink; 7.5 g $La_{0.5}Sr_{0.5}MnO_3$ (Seattle Speciality Ceramics), 7.5 g YSZ (Tosoh TZ10Y), 3.1 g 1,1,1-trichloroethane, 2.3 g methanol and 0.2 g glycerol trioleate milled for 4 h using zirconia media. The layer was applied by painting and was then dried at 150 °C. The LSM (Merck, $La_{0.88}Sr_{0.12}MnO_3$) cathode current collector was prepared from 20 g LSM, 24 g acetone, 0.6 g KD1 (Zeneca). This was milled for 5 h after which 4 g of terpineol was added. The acetone was removed by evaporation at 25 °C for 16 h. A layer was painted over the LSM/ZrO_2 and dried at 150 °C. Small reference electrodes were applied to the cathode side of the PEN tube at the same time. Cathodes were sintered between 1100 and 1300 °C for 1 h.

The particle size distribution of the inks was measured on a Malvern Laser particle size analyser using 1,1,1-trichloroethane as the solvent.

After firing the cells were assembled as follows. Wires, silver, Ni80Cr20 (both Advent), and Nimonic 90 (Ni53/Cr20/Co18/Fe5/Ti2.5/Al1.5 alloy wire) of diameters ranging from 0.125 to 0.5 mm were close wound (with each turn touching) over the cathode as the 'secondary' current collector (or interconnect). A 0.5 mm pure nickel wire was inserted into the tube as the anode current collect and interconnect. The pen tube and current collecting wire leads (70 mm long) were brought outside the furnace. The tube was also gas manifolded outside the furnace using a polyvinyl chloride (PVC) tubing. Before testing, the cells were heated to 900 °C in air, then reduced with 25 cm^3/min hydrogen bubbled through water at 25 °C.

The electrical characteristics of the cell were measured using a passive potentiostat [3]. Current–voltage (*I–V*) characteristics were determined by total cell voltage and current output. The cathode contribution to resistance was determined by the voltage difference between a sensing electrode next to the cathode winding and a small reference electrode next to the cathode. Because of the cell geometry, the cathode contribution contains a large proportion the *IR* drop in the zirconia. The contact resistance was determined from the voltage difference between the sensing electrode next to the cathode winding and the winding itself. Anode contributions were determined by the difference between the sum of the total cathode contribution (cathode contribution plus contact resistance) and cell voltage, and the open-circuit voltage. Unless otherwise stated, the cells were tested with a constant flow rate of 25 cm^3/min hydrogen.

PEN cells of 40 mm length were wound with 0.25 mm Ag, 0.25 and 0.5 mm Ni/Cr and 0.3 mm Nimonic 90. The cells were thermally cycled between 200 and 900 °C. The tubes were heated at 100 °C/min to 700 °C followed by 10 °C/min to 900 °C. Subsequently, the tubes were cooled at 100 °C/min to 200 °C. The tubes were subjected to at least 37 thermal cycles, periodically being measured for cell performance at 0.7 V. Cathode and contact contributions to resistance were measured as above. During the cycling, the total cell voltage was maintained at a constant 0.8 V by the passive potentiostat.

3. Results and discussion

The particle size distributions (vol.%) of the anode, cathode electrochemical layer and cathode current collect layer inks are shown in Fig. 1. The anode ink has a distribution with a mode of about 30 μm. This is due to the coarse, calcined YSZ used in its manufacture. There are no particles greater than the 108 μm sieve size. The significant volume of material below 1 μm in this distribution is likely to enhance the electrochemical properties of the anode. The LSM/YSZ ink has a large volume of sub-micron particles and displays a bimodal distribution, while the LSM current collector has an average particle size of 3 μm. The fine particles in the electrochemical layer should increase three-phase boundary area while the coarser particle size distribution in the pure LSM layer would be considered more suitable for current collection due to the higher in-plane conductivity of a coarse microstructure.

Table 1 shows the effect of operating temperature on the average specific performance of cathodes sintered between 1100 and 1300 °C with a 0.25 mm diameter silver wire as the

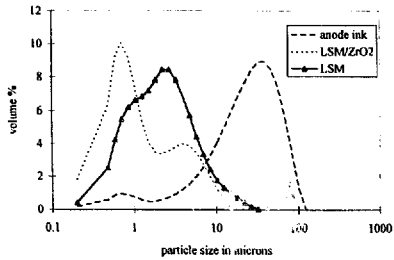

Fig. 1. Particle size distributions (vol.%) for anode and cathode inks.

Table 1
Average specific cell performance (mA/cm² at 0.7 V) for 5 mm long cells prepared from LSM/ZrO_2, Merck LSM cathode and standard anode sintered at various temperatures. Anode was sintered at 1300 °C before cathode was applied

Sintering temperature	Cell performance (mA/cm² at 0.7 V)	
°C)	800 °C	900 °C
1100	76	165
1200	102	221
1300	179	230

secondary cathode current collector. It is obvious that a higher sintering temperature significantly improves the specific current output of these 5 mm cells to an average maximum output of 230 mA/cm² at 0.7 V, 900 °C. While at lower temperatures the LSM/ZrO_2 layer is likely to remain relatively fine and have a large three-phase boundary. This does not appear to limit the performance of the cathode. The implication is that at higher firing temperatures, the increased density of the LSM/ZrO_2 electrochemical layer and LSM current collectors improves the in-plane and through-plane conductivity of the cathode. This leads to a lower cathode contribution to cell resistance and improved specific current output.

Fig. 2 shows the specific current output at 900 °C, 0.7 V for cells of various lengths prepared at 1300 °C from 3 and 8 mol% YSZ tubes. While the specific current of a short 4 mm long cell is acceptable, the performance drops rapidly with increasing cell length. This trend occurs in both the 3 and 8 mol% YSZ tubes. Increasing the proportion of Y_2O_3 in YSZ is known to improve oxygen ion diffusivity at 900 °C [4]. Since there appears to be little difference in current output between the two YSZs, it is apparent that the ionic conductivity of the YSZ does not limit the performance of the cells. Therefore, 3 mol% YSZ was the preferred electrolyte material because of its enhanced strength over 8 mol% YSZ.

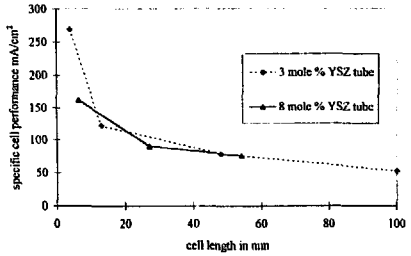

Fig. 2. Effect on specific cell performance (900 °C, 0.7 V total cell voltage) of various cell lengths (3 and 8 mol% YSZ tubes, standard anode, LSM/ZrO_2, LSM cathode 1300 °C).

Table 2 shows the electric properties for cells with different lengths prepared from 3 mol% YSZ tube shown in Fig. 2. The total power output increases from 57 to 275 mW for a 4 to 100 mm long cell. The specific cathode contribution to resistance (overvoltage and *IR* drops in cathode and some contribution from the YSZ electrolyte, but not *IR* drops in the metal interconnect) is seen to increase by a factor of three from a 4 to 48 mm cell. As the overvoltage current characteristics of the cathode might be assumed to be independent of cell length, this increase in specific cathode contribution is attributed to currents moving in the plane of the cathode (along the cell length). These currents are generated by potential differences along the cell and may be caused by a number of factors. The higher fuel utilisation for a given flow rate of hydrogen in longer cells generates more reaction products and hence a higher oxygen partial pressure. This causes a reduction in the Nernst potential and generates a potential difference along the cell. Other factors such as temperature differences along a longer cell may also contribute to cathode losses. However, as the measured temperature difference along a 100 mm cell was found to be only 10 °C, this can be neglected.

In Table 2 the specific contact resistance of a cell is seen to increase rapidly with the length. This contact resistance includes the lead resistance, the resistance at the electrode wire interface and the resistance of the wire coil itself. The Table shows that in long cells the resistance of an equivalent length of silver wire is small in relation to the total contact contribution. The resistance of an equivalent silver wire also neglects the fact that the wire turns are in contact and not insulated, so the current path may be significantly shorter.

Table 2
Properties of cells with various lengths at 900 °C, 0.7 V total cell voltage and 25 cm³/min hydrogen. Cells were sintered at 1300 °C and wound with 0.25 mm silver wire

Cell length	4 mm	13 mm	48 mm	100 mm
Cell current (mA/cm²)	269	122	78	52
Total cell current (mA)	81	120	283	391
Power output (mW)	57	84	200	275
Cathode contribution to resistance (Ω/cm²)	1.14	2.55	3.04	
Anode contribution to resistance (Ω/cm²)	0.24	0.2	0.43	
Contact resistance (Ω/cm²)	0.15	0.65	1.48	
Total contact resistance (Ω)	0.045	0.64	5.35	
Nos. turns Ag wire, approximative	16	52	192	400
Resistance of equivalent length silver wire (Ω)	0.0396	0.152	0.501	
Fuel utilisation (%)	2.2	3.3	7.8	10.8

Thus the resistance between the wire and the LSM current collector obviously dominates contact contribution. While specific cathode and contact resistances are affected by cell length, the anode contribution appears to be independent of length and the differences seen are probably attributable to the difficulty in achieving consistency in the anode wire current collect between different cells.

Fig. 3 shows the specific current output of various length cells at different fuel utilisations. For the longest (100 mm) cell the specific current output drops below 50 mA/cm^2 at 50% fuel utilisation. This drop is to about 70% of the performance at low utilisations. This corresponds to a flow rate of 5 cm^3/min of hydrogen. The reduction in cell output is explained by the reduction in Nernst potential as the oxygen partial pressure increases in the fuel stream due to reaction. While the reduction in performance is significant at high utilisations its magnitude is much smaller than that caused by increasing the length of cell. High utilisations can be achieved in these small diameter tubes by making longer cells but only at the expense of significantly lower specific current outputs.

The short-term performance of a 36 mm length cell wound consecutively with 0.25 mm silver, Ni/Cr, (0.125 to 0.5 mm) and 0.3 mm Nimonic 90 wires are shown in Fig. 4. The 0.25 mm silver winding shows the best overall specific current output, while the slightly thicker Nimonic winding gave 80% of this performance for a single winding. The Ni/Cr output showed a dependence on the diameter of the wire, with a thick wire being best. However, the reduction in performance of the 0.125 mm Ni/Cr wire over 0.5 mm Ni/Cr wire is only by a factor of 4, whereas the difference between the resistances of the equivalent lengths of Ni/Cr wire would be of the order of 100 (206 to 3.3 Ω approximately). This is an indication that contact resistance dominates the loss in wire windings. That the Nimonic 90 winding gives better performance than a thicker Ni/Cr wire indicates that there is a lower contact resistance between this wire material and the LSM surface. Winding a second coil over the top of the first gave a small increase in current output by shorting across the inner turns to further reduce coil resistance.

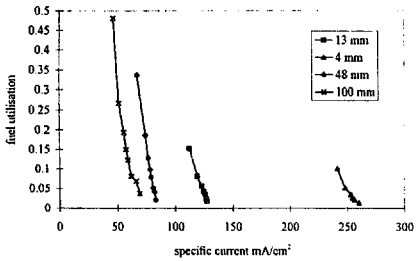

Fig. 3. Effect of increasing fuel utilisation on specific cell performance at 900 °C, 0.7 V (3 mol% YSZ tubes, standard anode, LSM/ZrO_2, LSM cathode 1300 °C).

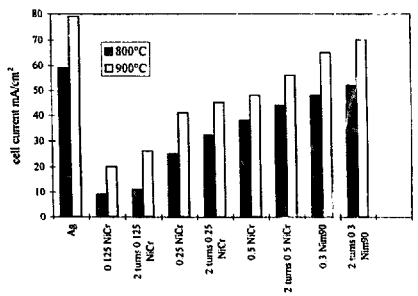

Fig. 4. Specific cell performance (36 mm cell) with various base metal windings at 900 °C, 0.7 V.

Fig. 5 shows the *I–V* characteristics, total cathode contribution to resistance and the contact contribution to resistance of 40 mm long, 0.25 mm diameter silver and Ni/Cr windings. For the silver winding, it can be seen that the contact resistance (the interfacial resistance between the LSM and the wire, the coil resistance and the lead resistance) accounts for some 30% of the total resistance of the cathode. In contrast to this, for a single 0.25 mm diameter Ni/Cr wire the contact contribution accounts for 90% of the total cathode resistance.

Fig. 6 shows the specific cell output of 40 mm cells wound with 0.25 mm Ag, 0.25 and 0.5 mm Ni/Cr and 0.3 mm Nimonic 90 versus the number of thermal cycles. While the performance of the silver wound cell remains constant, all the base metal windings degraded rapidly. A large degradation was seen to occur in all the cells after a gas failure at 35 cycles (the cells were commonly manifolded). This is most likely to be due to damage to the anode caused by oxidation and subsequent reduction. This is confirmed in Fig. 7 which shows the cathode and contact contributions of the 0.25 mm Ag, 0.5 mm Ni/Cr and 0.3 mm Nimonic 90 wires. While a reduction in performance occurred after 35 cycles, no change is seen in the cathode or contact contributions for the silver wire. The reduction in performance of the base metal wind-

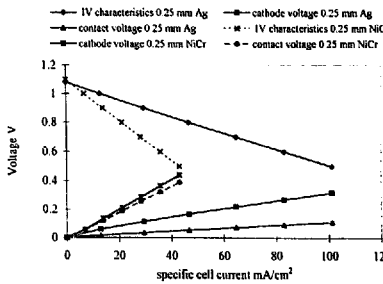

Fig. 5. *I–V* characteristics, cathode and contact contributions to cell resistance for 0.25 mm Ag and Ni/Cr wound cells (TZ3Y tube, LSM/ZrO_2, LSM, standard anode, 40 mm cell length, 900 °C, 0.7 V).

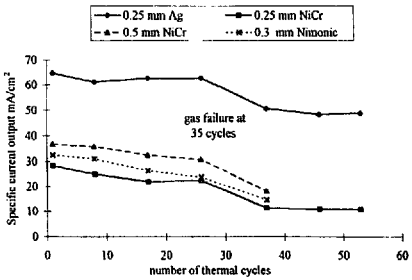

Fig. 6. Specific current output for 40 mm cells (at 900 °C, 0.7 V) wound with 0.25 mm Ag, 0.25 and 0.5 mm Ni/Cr and 0.3 mm Nimonic 90 wires during thermal cycling.

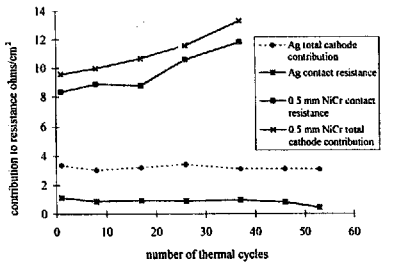

Fig. 7. Cathode and contact contributions to cell resistance for 40 mm cells (at 900 °C, 0.7 V) for 0.25 mm Ag and 0.5 mm Ni/Cr wound cells during thermal cycling.

ings is due purely to an increase in contact resistance. This is attributed simply to the continued oxidation of the alloys at elevated temperatures.

4. Conclusions

A specific current output of about 250 mA/cm² at 900 °C, 0.7 V was achieved in 5 mm long cells. Specific performance dropped rapidly with increasing length of cell. The reduction in specific performance was attributed to an increase in both the specific resistance of the cathode and the increase in the specific contact resistance with cell length. The contact contribution to cell resistance was dominated by contact resistance between the wire and the LSM. Fuel utilisations of up to 50% were tested in 100 mm cells. Cell output was of the order of 50 mA/cm² at 0.7 V and 900 °C. Various base metal windings were compared with the 0.25 mm silver wire current collector. Larger diameter wires were found to have significantly improved performance over smaller diameters. A Nimonic 90 winding achieved 80% of the performance of an equivalent silver winding in short-term tests. Fifty three cycles between 200 and 900 °C produced no degradation due to thermal shock in silver wound cells. Cell output with base metal windings degraded, due to an increase in the contact contribution to resistance of the wires.

Acknowledgements

The author would like to thank EPSRC for provision of funding for this work, I. Rouse (Pikem) for cathode materials and Sapco for supplying the YSZ tubes.

References

[1] W. Winkler, in U. Bossel (ed.), *Proc. 1st European Solid Oxide Fuel Cell Forum, Lucerne, Switzerland, 3–7 Oct. 1994.*
[2] K. Kendall and M. Prica, in U. Bossel, *Proc. 1st European Solid Oxide Fuel Cell Forum, Lucerne, Switzerland, 3–7 Oct. 1994.*
[3] R.C. Copcutt, Determination of solid electrolyte performance characteristics using current interruption, *Paper presented at Electrochem '95, University of Wales, Bangor, UK, 10–14 Sept. 1995.*
[4] B.C.H. Steele, in U. Bossel, *Proc. 1st European Solid Oxide Fuel Cell Forum, Lucerne, Switzerland, 3–7 Oct. 1994.*